UDK 544.163.2 : 544.228

A.E. Grechanovsky, A.B. Brik, O.M. Ponomarenko

INFLUENCE OF STRUCTURE, CHARACTER OF CHEMICAL BONDING AND ELASTIC PROPERTIES ON THE RADIATION STABILITY OF SILICATES, PHOSPHATES AND METAL OXIDES DEDUCED BY COMPUTER SIMULATIONS

The radiation stability of periclase MgO, rutile TiO_2, zircon $ZrSiO_4$, xenotime YPO_4, quartz SiO_2, cristobalite SiO_2, gallium phosphate $GaPO_4$ and fluorapatite $Ca_{10}(PO_4)_6F_2$ has been studied by computer simulations methods. The number of Frenkel pairs after propagation of the primary knock-on atom of thorium with a kinetic energy of 10 keV has been characterized by molecular dynamics method. Calculation of chemical bonds covalency degree in studied minerals has been performed using the self-consistent SIESTA method, an implementation of the density functional theory. Calculation of the effective charge of oxygen atoms has been performed using *ab initio* Hartree-Fock method and *B3LYP* hybrid functional. It is established that the radiation stability of these minerals depends significantly on the structure topology (the connectivity index, the number of different polyhedra, connected in oxygen positions and the number of nonequivalent positions of oxygen atoms and cations in a structure). Besides, the radiation stability of silicates and metal oxides can be mainly characterized by the effective charge of oxygen atoms. It has been shown, that bulk modulus also influences on radiation stability of silicates with related structures.

E-mail: grechanovsky@igmof.gov.ua

Introduction. Nuclear power production was increased in some countries (including Ukraine) in the last decades. The "Strategy of the nuclear power industry development" [20] assumes that the nuclear power plant share in the total national power generation reached in 2005 will be maintained on the same level during the period of 2006 to 2030 (this is about a half of the total annual electric power generation in Ukraine). On the basis of the preliminary estimation of electric power generation increasing in 2.2 times during this period it has been offered both extension of the service life of existing and construction of new facilities at the nuclear power plants. Therefore for stable and progressively development of the nuclear power engineering a decision of some

problems, related to long-term storage of high level wastes (HLW) is needed.

So, the future of nuclear power engineering is linked to our ability to effectively handle a nuclear waste. Vitrification, or immobilization of the nuclear waste in glass, has been and remains to be a popular way of its handling. But the operating period of glass matrices is about 40—50 years only. The effective alternative to vitrification has been immobilization of HLW in ceramic matrices and minerals. The central question is how effective a matrix will remain as a barrier over the required period of time, which for various isotopes varies from tens to tens of thousands years.

For explaining different radiation stability of different minerals and technical materials some criteria have been offered in literature, one of which relates radiation stability to the ability to form glass by liquid quenching [19], second crite-

30

ISSN 0204-3548. Mineral. Journ. (Ukraine). 2009. 31, No 4

rion relates radiation stability to the "structure topology" [5], third — with degree of chemical bonds covalency in studied minerals [3, 4, 13, 17], fourth — with certain physical properties, such as a polymerization degree of mineral structures and bulk modulus of minerals [2]. In spite of considerable successes, many questions are not studied enough in this area of knowledge. It belongs, in particular, to finding out principles which determine radiation stability of minerals.

The purpose of this research is an attempt to find relation between the radiation stability of phosphates, silicates and metal oxides and characteristics of its crystalline structures.

Methods. The radiation stability of minerals was studied by molecular dynamics simulation method (MD simulation method). This method consists in calculation of atoms trajectories in a simulation box, using Newton's second law of motion. Initial coordinates and velocities of the atoms, and also interatomic potentials are set as initial data. We have used the following interatomic potentials for studied minerals:

a) Buckingham potential in the form

$$V(r) = A \cdot \exp(-r/\rho) - C \cdot r^{-6}, \qquad (1)$$

with the parameters r — the distance between two atoms (Å), A — the pre-exponential factor for the repulsive part of the potential (eV), ρ — the hardness parameter (Å), C — the force parameter for Van der Waals interaction (eV $\cdot$ Å^6);

b) Potential of Morse in the form

$$V(r) = D \cdot \big[\exp(-2\alpha(r - r_0)) - 2\exp(-\alpha(r - r_0))\big], \qquad (2)$$

with the parameters r — the distance between two atoms (Å), D — the dissociation energy of the bonding atoms (eV), α — the softness parameter (Å^{-1}), r_0 — the bond distance between the atoms (Å). The parameters, appearing in (1) and (2) were taken from the works [3, 15, 17]. To establish these parameters optimization of the structures was performed using the experimental values of unit-cell parameters, bond lengths, bond angles, elastic constants and bulk modulus of studied minerals.

As a recoil atom for the nanofragments of simulated minerals, containing about $2 \cdot 10^5$ atoms we have used the primary knock-on atom (PKA) of thorium with energy of 10 keV. At such energies the number of Frenkel pairs increases in proportion to the PKA energy [1]. Therefore from methodological and practical points of view (limited computational power) using the PKA with

energy of 10 keV is rational, in spite of the fact that the real energy of a thorium recoil atoms is about to 70 keV. For interatomic distances smaller than 1Å, the pair potentials were fitted to the strong repulsive ZBL potentials [17]. On the preliminary stage of the simulations all structures were brought to the state of thermal equilibrium during 10 ps at 300 K using the NPT ensemble (constant pressure, temperature and number of atoms). The main stage of the simulations is performed using the NVE microcanonical ensemble (constant volume, energy and number of atoms). All MD simulations were performed using the DL_POLY molecular simulation package [17], designed to facilitate the molecular dynamics simulations of macromolecules, polymers, ionic systems and minerals.

For the calculation of the degree of chemical bonds covalency in studied minerals we have used the self-consistent SIESTA method [11], an implementation of the density functional theory (DFT) [6]. The electronic density was obtained using the exchange-correlation potential of Perdew in the Perdew-Burke-Ernzerhof parametrization [12], and normconserving pseudopotentials in the Kleinman-Bylander form [8], to remove the core electrons from the calculations. The Kohn-Sham eigenstates were expanded in a localized basis set of numerical orbitals, calculated by the Numerov numerical method [7]. We have used a split-valence basis sets [11] during these quantum-chemical calculations.

For the calculation of the effective charge of oxygen atoms in the minerals we have performed *ab initio* calculations by the Hartree-Fock method [14] using the *B3LYP* hybrid functional [3, 13] (density functional theory). We have used the PC GAMESS code [10] for this purpose. The parameters of atoms basis sets are shown in Table 1: 1 — the atom type, 2 — the number and the types of

Table 1. **Parameters of basis sets, used in Hartree-Fock calculations**

Atom type	Gaussian primitives	Shells
Mg	15s, 7p	1s, 3sp
O	14s, 6p, 2d	1s, 3sp, 2d
Ti	20s, 12p, 3d	1s, 3sp, 1d
Si	15s, 9p, 1d	1s, 3sp, 1d
P	16s, 8p, 1d	1s, 3sp, 1d
Ga	21s, 13p, 5d	1s, 5sp, 2d
Ca	21s, 13p, 3d	1s, 4sp, 1d
Zr	26s, 17p, 9d	1s, 4sp, 3d
Y	26s, 17p, 10d	1s, 4sp, 3d

Table 2. **Characteristics of studied minerals and results of MD simulations and DFT simulations of the minerals**

Mineral and its chemical formula	Parameters, which characterize the mineral structures			Results of MD- and DFT simulations			T_c, K
	Space group	Connectivity	G, GPa	$Q(X{-}O)$, $|e|$	$\dfrac{N_F}{D_F(\text{Å})}$	$\dfrac{N_{max}}{D_{min}(\text{Å})}$	
Periclase MgO	$Fm3m$	O—6Mg	240	-0.11 (X = Mg)	$\dfrac{30}{5}$	$\dfrac{1280}{71}$	20
Rutile TiO$_2$	$P4_2/mnm$	O—3Ti	237	-0.35 (X = Ti)	$\dfrac{490}{54}$	$\dfrac{6230}{90}$	205
Zircon ZrSiO$_4$	$I4_1/amd$	O—2Zr, Si	222	-0.6 (X = Si) -0.29 (X = Zr)	$\dfrac{820}{28}$	$\dfrac{6600}{62}$	1000
Xenotime YPO$_4$	$I4_1/amd$	O—2Y, P	147	-0.61 (X = P) -0.25 (X = Y)	$\dfrac{790}{67}$	$\dfrac{7220}{99}$	428
Quartz SiO$_2$	$P3_221$	O—2Si	33	-0.61 (X = Si)	$\dfrac{2220}{128}$	$\dfrac{4430}{136}$	1400
Cristobalite SiO$_2$	$P4_12_12$	O—2Si	16	-0.62 (X = Si)	$\dfrac{3240}{114}$	$\dfrac{6510}{120}$	—
Gallium phosphate GaPO$_4$	$P3_221$	O1—Al, P O2—Al, P	40	-0.59 (X = P) -0.57 (X = Ga)	$\dfrac{3240}{143}$	$\dfrac{5650}{143}$	650
Fluorapatite Ca$_{10}$(PO$_4$)$_6$F$_2$	$P6_3/m$	O1—2Ca1, P, Ca2 O2—2Ca1, P, Ca2 O3—Ca1, P, 2Ca2	99	-0.64 (X = P) -0.08 (X = Ca)	$\dfrac{1690}{131}$	$\dfrac{15260}{132}$	475

gaussian primitives, 3 — the number and the types of shells, corresponding to these primitives (for example record "2d" indicates that some GTOs combines in two d-shells).

We have used the connectivity index as a parameter, which characterizes influence of mineral structure topology on its radiation stability. This parameter is determined as the number of polyhedrons, connected in oxygen atoms positions.

Results and discussion. The results of performed MD- and DFT simulations are given in Table 2. The following quantities are indicated in this table: 1 — the mineral and its chemical formula; 2 — the

Table 3. **Results of Hartree-Fock calculations of studied minerals**

Mineral and its chemical formula	Methodology	$Q(O)$, $|e|$	$Q(O)$, $|e|$ [18]
Periclase MgO	Embedded cluster	-1.96	-1.86
Rutile TiO$_2$	[Ti$_3$O$_{14}$]$^{-16}$ cluster	-1.29	-1.26
Zircon ZrSiO$_4$	[Zr$_5$Si$_6$O$_{44}$]$^{-44}$ cluster	-1.06	—
Xenotime YPO$_4$	[Y$_5$P$_6$O$_{44}$]$^{-43}$ cluster	-0.96	—
Quartz SiO$_2$	[Si$_5$O$_{16}$H$_{12}$] cluster	-0.79	-0.78
Cristobalite SiO$_2$	[Si$_6$O$_{18}$H$_{12}$] cluster	-0.78	—
Gallium phosphate GaPO$_4$	[Ga$_3$P$_3$O$_{18}$H$_{12}$] cluster	-0.92	—
Fluorapatite Ca$_{10}$(PO$_4$)$_6$F$_2$	[Ca$_9$P$_6$O$_{27}$]$^{-6}$ cluster	-1.18	—

space group of mineral; 3 — the connectivity of mineral structure, which characterizes the number and the types of polyhedrons, connected in oxygen atoms positions; 4 — the bulk modulus G, which characterize the pressure ΔP needed for the relative compression of a mineral on a value of $\Delta\varepsilon = \Delta V/V$ ($G = \Delta P/\Delta\varepsilon$); 5 — the value of the electrons charge, localized between X and O atoms, which characterizes the degree of chemical X—O bond covalency; 6 — the number of Frenkel pairs N_F and the linear size of a displacements cascade D_F after defects annealing; 7 — the maximum number of Frenkel pairs N_{max} and the linear size of a displacements cascade D_{max} before defects annealing; 8 — the critical temperature of amorphisation T_c (if $T > T_c$, then a mineral cannot be amorphized). Quantities from cl. 3 are given from the structural data, cl. 4 — from the experimental data [3, 15, 17], cl. 5—7 — from the results of this study (MD- and DFT simulations), cl. 8 — from the ion-beam irradiation experiments with 800 keV $\div$ 1.5 MeV Kr$^+$ ions [9, 17].

The results of performed Hartree-Fock study of the minerals (the effective charge of oxygen atoms $Q(O)$) are given in Table 3. The ionic nature of the periclase structure implies that the Madelung potential must be included in the quantum-chemical calculations. Indeed, several properties of MgO are incorrectly described if the long-range
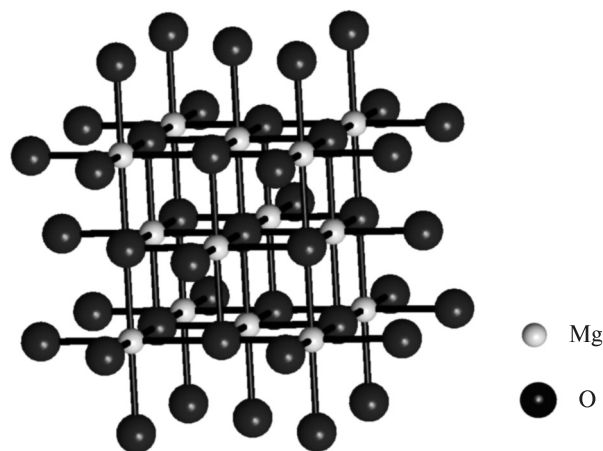
32

ISSN 0204-3548. Mineral. Journ. (Ukraine). 2009. 31, No 4

Fig. 1. Periclase structure

Coulomb interactions are not taken into account. To provide a simple representation of these interactions we have used $[Mg_7O_6]^{2+}$ fragment, embedded in large arrays of $\pm 2\,|e|$ point charges. For rutile, zircon, xenotime and fluorapatite structures we have used respectively $[Ti_3O_{14}]^{-16}$, $[Zr_5Si_6O_{44}]^{-44}$, $[Y_5P_6O_{44}]^{-43}$ and $[Ca_9P_6O_{27}]^{-6}$ clusters. Using of larger clusters was restricted due to limited computational power. In quartz, cristobalite and gallium phosphate clusters (respectively $[Si_5O_{16}H_{12}]$, $[Si_6O_{18}H_{12}]$ and $[Ga_3P_3O_{18}H_{12}]$) dangling bonds have been saturated by H atoms, common procedure to terminate clusters of covalent materials [16]. The positions of H atoms were fixed at a distance of 0.96 Å from the respective O atoms along the O−Si and O−Ga directions. The position of all Si, Ga and O atoms of the cluster has been reoptimised. Electrostatic energy was taken into account for all quantum-chemical calculations. Urusov et al. data [18], obtained by means of the minimization of cohesive energy as the function of the oxygen atoms charge for three minerals (periclase, rutile, quartz), are also given in Table 3 for comparison of our results with other data.

In the case of periclase (*F*m3m space group) the connectivity index of the structure (Fig. 1) is equal to $C = 6$. Such high value of the connectivity index agreed with a low degree of Mg−O bond covalency ($Q(Mg-O) = -0.11\,|e|$), with a high value of oxygen charge ($Q(O) = -1.96\,|e|$), and also with considerable radiation stability of this mineral (the number of Frenkel pair at the end of simulation $N_F = 30$ and the critical temperature of amorphization $T_c = 20$ K). The periclase structure is characterized by a high value of the bulk modulus ($G = 240$ GPa), however the size of displace-

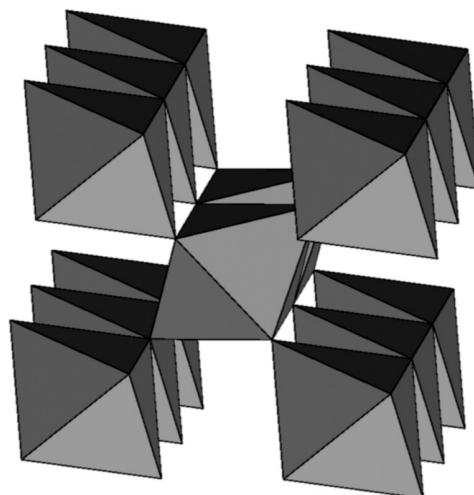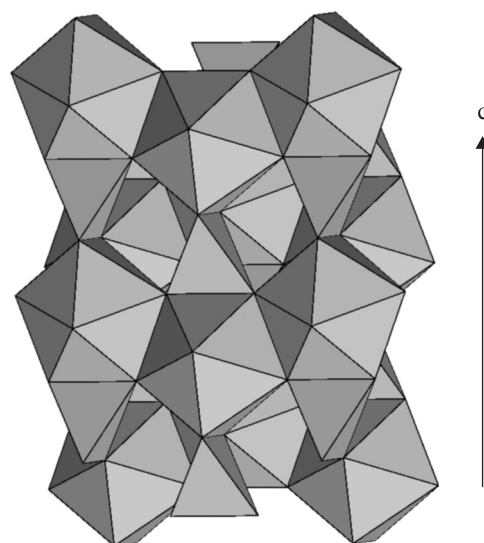*Fig. 2.* Rutile structure

Fig. 3. Zircon structure

ments cascade before defects annealing $D_{max} = 71$Å due to the presence of nanochanels in the structure.

Rutile ($P4_2/mnm$ space group) is characterized by the connectivity index $C = 3$ (Fig. 2). From other hand, the degree of chemical bonds covalency is higher ($Q(Ti-O) = -0.35\,|e|$) and the oxygen charge is less ($Q(O) = -1.29\,|e|$) in compare with periclase structure. So, the radiation stability of rutile structure is less in compare with periclase structure both from the experimental data ($T_c = 205$ K for rutile and $T_c = 20$ K for periclase) and from the MD simulations data ($N_F = 490$ for rutile and $N_F = 30$ for periclase). In spite of identical values of the bulk modulus of two minerals ($G \approx 240$ GPa) rutile is characterized by a larger li-
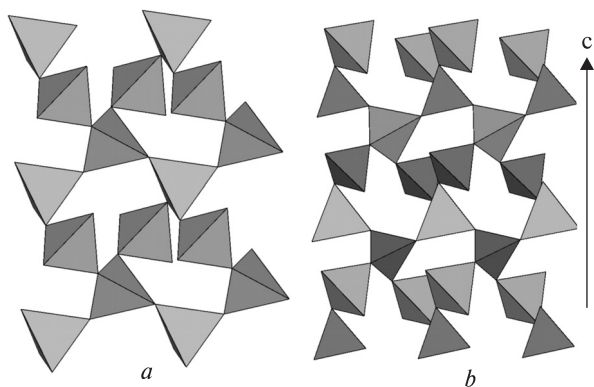
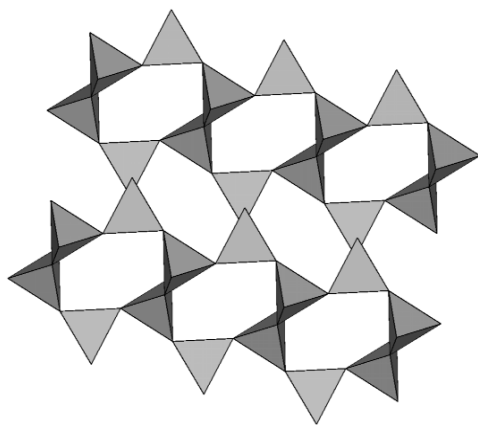*Fig. 4.* Quartz (*a*) and gallium phosphate (*b*) structures

Fig. 5. Cristobalite structure

near size of displacements cascade ($D_{max} = 90$ Å) in compare with periclase.

Zircon and xenotime structures (Fig. 3) with $I4_1/amd$ space group are determined by the alternating edge-sharing $[AO_8]$ dodecahedrons (A = = Zr, Y) and $[BO_4]$ tetrahedrons (B = Si, P) forming chains parallel to the (001) axis. The connectivity index of these structures is $C = 3$, however unlike previous structures two AO_8 polyhedrons and one BO_4 tetrahedron are combine in every oxygen atom positions. From other hand, these structures are characterized by a large degree of chemical bonds covalency (Q(Si−O) = -0.6 |e| for zircon and Q(P−O) = -0.61 |e| for xenotime), and a small value of the oxygen charge (-1.06 |e| for zircon and -0.96 |e| for xenotime). These results agree with the radiation stability of zircon and xenotime, obtained from the MD simulation data ($N_F = 820$ for zircon and $N_F = 790$ for xenotime). In spite of this, the radiation stability from the MD simulation data for xenotime does not agree with the experimental data ($T_c = 1000$ K for zircon and $T_c = 428$ K for xenotime). This disagreement will be discussed below.

A less value of the oxygen charge in xenotime than one in zircon correlates with a higher value of the maximum number of Frenkel pairs in xenotime in compare with zircon ($N_{max} = 7220$ for xenotime and $N_{max} = 6600$ for zircon). Besides, for higher values of the PKA energy (the PKA energy is more than 10 keV) it can result in a higher value of the number of Frenkel pairs in xenotime in compare with zircon after defects annealing. It should be also note that displacements cascade in xenotime has a larger sizes in compare with zircon ($D_F = 28$ Å for zircon and $D_F = 67$ Å for xenotime) due to a less bulk modulus in xenotime than one in zircon.

Next two minerals (quartz and cristobalite) have a low radiation stability. In the case of quartz structure (Fig. 4, *a*) with $P3_221$ space group and cristobalite structure (Fig. 5) with $P4_12_12$ space group the connectivity index is equal $C = 2$. In addition, the degree of Si−O bond covalency is Q(Si−O) $\approx$ ≈ -0.6 |e| and the oxygen charge is Q(O) $\approx$ ≈ -0.8 |e| for both structures. However, the radiation stability of cristobalite less than one of quartz because the bulk modulus in cristobalite less ($G =$ $= 16$ GPa) in compare with quartz ($G = 33$ GPa).

Gallium phosphate structure (Fig. 4, *b*) with $P3_221$ space group is determined by the alternating PO_4 and GaO_4 tetrahedrons, spiraling along the three-two screw c-axis. PO_4 and GaO_4 tetrahedrons are characterized by approximately equal covalency degree of P−O and Ga−O chemical bonds (Q(P−O) = -0.59 |e| and Q(Ga−O) = $= -0.57$ |e|), and the $GaPO_4$ oxygen charge has even a higher value in compare with quartz. But, for the gallium phosphate structure a different tetrahedrons (PO_4 and GaO_4) are combined in every oxygen position. Consequently this material has a less radiation stability than quartz from the MD simulation data ($N_F = 3240$ for $GaPO_4$ and $N_F = 2220$ for quartz), in spite of the fact that the bulk modulus in $GaPO_4$ even more, than in quartz. However, as well as in the case of xenotime, the radiation stability of gallium phosphate from the MD simulation data does not agree with the experimental data ($T_c = 650$ K for $GaPO_4$ and $T_c =$ $= 1400$ K for quartz).

The last investigated mineral is fluorapatite with $P6_3/m$ space group. In this mineral (Fig. 6) the connectivity index is equal $C = 4$. However, the process of defects annealing in a displacements cascade is complicated due to a difficult structure of fluorapatite (presence of three nonequivalent oxygen positions (O1, O2, O3) and two nonequi-

34

valent calcium positions (Ca1, Ca2)), large degree of P—O bond covalency (Q(P—O) = -0.64 |e|) and significant mobility of fluorine atoms. So, $N_F = 1690$ from the MD simulation data. However, as well as for others phosphate minerals, the radiation stability of fluorapatite from the MD simulation data does not agree with the experimental data ($T_c = 475$ K). It should be also noted, that a low value of the bulk modulus for fluorapatite ($G = 99$ GPa) agrees with significant size of a displacements cascade ($D_F = 131$ Å).

We paid attention in this article that the radiation stability of phosphate minerals, obtained from the MD simulation data does not agree with the experimental data. This disagreement connected with the fact, that MD simulations have nanoseconds time-limit even for modern supercomputers. Defects annealing in a displacements cascade takes place during nanoseconds. However, after this time the radiation-enhanced recrystallization of amorphous zones takes place during significantly longer time scale.

In the case of silicates the activation energy of the radiation-enhanced recrystallization of amorphous zones has a large value $E_a \approx 3$ eV [9] and the recrystallization does not take place at the moderate temperatures ($T \approx 500$ K) even during the geological time. Therefore the radiation stability of silicates obtained from the MD simulation data agrees with the experimental data. For phosphates this energy is $E_a \approx 1 \div 1.5$ eV [9] and even at the moderate temperatures ($T \approx 500$ K) the recrystallization takes place very rapidly (in some cases during a seconds). In this case the MD simulation data reflect the number of Frenkel pairs, remaining in a structure after defects annealing in a displacements cascade. However, in the case of consideration of phosphates separately from silicates and metal oxides its radiation stability, obtained from the MD simulation data correlates with the experimental data — the critical temperature of amorphization decreases with decreasing the number of Frenkel pairs in phosphates.

Our methods and approaches can be used for the decision of practical tasks. So, zircon-bearing rare-earth garnetiferous matrix ($Ca_{3-x}A_x$)× ×($Zr_{2-y}Fe_y$) Fe_3O_{12} (A = Ce, Th, La, Gd, Sr) was successfully synthesized in the Institute of environmental geochemistry of the National Academy of Sciences and Ministry of Emergencies of Ukraine. Gamma-irradiation of matrices samples was performed up to doses $2.3 \cdot 10^7$ Gy for the verification of its radiation stability. The matrices

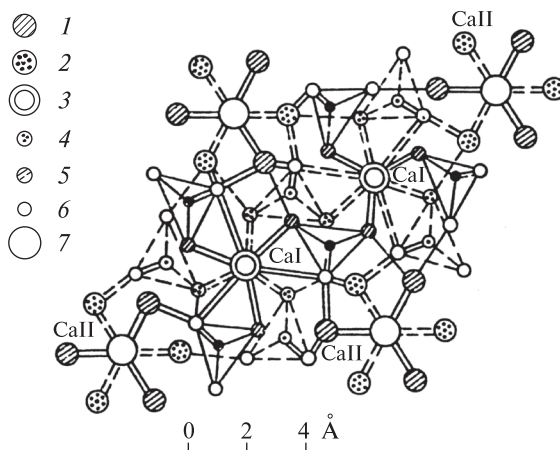*Fig. 6.* Fluorapatite structure: *1* — Ca on $\frac{1}{4}$ c; *2* — Ca on $\frac{3}{4}$ c; *3* — Ca on 0, $\frac{1}{2}$ c; *4* — O on $\frac{3}{4}$ c; *5* — O on $\frac{1}{4}$ c; *6* — O on $\frac{1}{20}$, $\frac{3}{20}$ c etc.; *7* — F on $\frac{1}{4}$, $\frac{3}{4}$ c.

samples remain in the crystalline state at such doses. From other hand, it is also important to investigate the matrices response on α-recoil atoms motion for the estimation of its radiation stability. Performing of heavy ion-beam irradiations of matrices needed for these investigations is impossible for our researchers at present. However such tasks can be decided by our computer simulations.

Conclusions. The results of researches show that the radiation stability of minerals caused by various factors. In the case of metal oxides (periclase, rutile) two main factors are following: the connectivity index and the degree of chemical bonds covalency of the structures (or effective charge of oxygen atoms). In the case of silicates (zircon, quartz, cristobalite) one more factor which influences on its radiation stability is the value of bulk modulus. Displacements cascades in minerals with a higher values of the bulk modulus are characterized by a less value of longitudinal dimensional and respectively these minerals are characterized by more radiation stability than minerals with a less value of the bulk modulus (these minerals must have related structures and close degrees of chemical bonds covalency).

It should be noted that for metal oxides and silicates the connectivity index and the effective charge of oxygen atoms are interconnected. Structures with a large connectivity index (periclase, rutile) are characterized by large values of both the effective charge of oxygen atoms and the radiation stability. Structures with a small connectivity index (quartz, cristobalite) are characterized by small values of both the effective charge of oxy-

gen atoms and the radiation stability. In simple terms, the relevance of the type of interatomic forces for resistance to amorphization can be discussed as follows. After the displacement of atoms by propagating heavy ion, the rearrangement of atoms needed to regain coherence with the crystalline lattice involves significant atomic motion. In a covalent structure, the interactions can be thought of as short-range directional constraints, due to the substantial electronic charge being localized between the neighbouring atoms. Therefore cooperative atomic motion is "hooked" by the electrons between neighbouring atoms, and requires breaking directional covalent bonds with associated energy cost. On the other hand, highly ionic structure can be viewed as a collection of charged ions. The cooperative rolling of spheres which are only electrostatically charged, does not require additional activation energy, giving damaged ionic structure better chances to re-establish coherence with crystalline lattice.

Unlike silicates which are characterized by almost full absence of the radiation-enhanced recrystallization of amorphous zones at the moderate temperatures ($T \approx 500$ K), this process takes place very rapidly in phosphates for these temperatures (in some cases during a seconds). However, in spite of peculiarities of phosphate structures, the radiation stability of phosphate minerals is influenced mainly by the connectivity index, the effective charge of oxygen atoms and "structure complication" (the number of different polyhedra, connected in oxygen positions, and the number of nonequivalent positions of oxygen atoms and cations in the structure).

So, fluorapatite structure is characterized by a higher connectivity index ($C = 4$) as compared to xenotime structure ($C = 3$). However, fluorapatite structure is more complicated, than xenotime structure. So, the radiation stability of fluorapatite structure is a less in compare with xenotime structure ($T_c = 428$ K for xenotime and $T_c = 475$ K for fluorapatite). In the case of gallium phosphate $GaPO_4$ the connectivity index is equal $C = 2$. So, the radiation stability of this material is a less ($T_c = = 650$ K) in compare with fluorapatite or xenotime.

Results of this study can be used for solving fundamental and practice tasks connected with immobilization and disposal of a high-level waste. In particular, these results can be used for the assessment of radiation stability of matrices, proposed for immobilization of the high-level waste. Our computer simulations permit to analyze and predicted matrices reliability under radiation damage. Using computer simulation methods can save timing and money budgets and promotes to choice of the appropriated matrix.

1. *Devanathan R., Corrales L.R., Weber W.J. et al.* Molecular dynamics simulation of defect production in collision cascades in zircon // Nucl. Instrum. and Meth. in Phys. Res. B. — 2005. — **228**. — P. 299—303.
2. *Eby R.K., Ewing R.C., Birtcher R.C.* Amorphization of complex silicates by ion-beam irradiation // J. Mater. Res. — 1992. — **7**, No 11. — P. 3080—3102.
3. *Grechanovsky A.E.* The influence of structure and chemical bonding on the radiation stability of U-, Th-minerals : dis. cand. phys.-math. sci. / M.P. Semenenko In-te of Geochemistry, Mineralogy and Ore Formation of the NAS of Ukraine. — Kyiv, 2008. — 152 p. — Typing (in Russian).
4. *Grechanovsky A.E., Brik A.B., Ponomarenko A.N., Kalinichenko A.M.* Mechanisms of formation and properties of nano-sized systems in metamict zircons // Mineralogical Intervention in Micro- and Nanoworld : Materials of Intern. miner. sem. — Syktyvkar : Geoprint, 2009. — P. 194—196 (in Russian).
5. *Hobbs L.W.* The role of topology and geometry in the irradiation-induced amorphization of network structures // J. Non-Cryst. Sol. — 1995. — **182**, No 1. — P. 27—39.
6. *Hohenberg P., Kohn W.* Inhomogeneous Electron Gas // Phys. Rev. B. — 1964. — **136**, No 3. — P. 864—871.
7. *Junquera J., Paz O., Sanchez-Portal D., Artacho E.* Numerical atomic orbitals for linear-scaling calculations // Ibid. — 2001. — **64**, No 23. — P. 235111.
8. *Kleinman L., Bylander D.M.* Efficacious Form for Model Pseudopotentials // Phys. Rev. Lett. — 1982. — **48**, No 20. — P. 1425—1428.
9. *Meldrum A., Boatner L.A., Ewing R.C.* A comparison of radiation effects in crystalline ABO4-type phosphates and silicates // Miner. Mag. — 2000. — **64**, No 2. — P. 185—194.
10. *Nemukhin A.V., Grigorenko B.L., Granovsky A.A.* Molecular modelling by using the PC GAMESS program : From diatomic molecules to enzymes // Chem. Bull. Moscow Univ. — 2004. — **45**, No 2. — P. 75—102.
11. *Ordejon P., Artacho E., Soler J.M.* Self-consistent order-N density-functional calculations for very large systems // Phys. Rev. B. — 1996. — **53**, No 16. — P. R10441—R10444.
12. *Perdew J.P., Burke K., Ernzerhof M.* Generalized Gradient Approximation Made Simple // Phys. Rev. Lett. — 1996. — **77**, No 18. — P. 3865—3868.
13. *Ponomarenko A.N., Brik A.B., Grechanovsky A.E. et al.* Physical Models, Investigation Methods and Properties of Metamict Zircons // Mineral. Journ. (Ukraine). — 2009. — **31**, No 2. — P. 20—38 (in Russian).

36

ISSN 0204-3548. Mineral. Journ. (Ukraine). 2009. 31, No 4

14. *Pople J.A., Nesbet R.K.* Self-Consistent Orbitals for Radicals // J. Chem. Phys. — 1954. — **22**, No 3. — P. 571—572.

15. *Rabone J.A.L., Carter A., Hurford A.J., de Leeuw N.H.* Modelling the formation of fission tracks in apatite minerals using molecular dynamis simulations // Phys. Chem. Miner. — 2008. — **35**, No 10. — P. 583—596.

16. *Sauer J., Ugliengo P., Garrone E., Saunders V.R.* Theoretical Study of Van der Waals Complexes at Surface Sites in Comparison with the Experiment // Chem. Rev. — 1994. — **94**, No 7. — P. 2095—2160.

17. *Trachenko K., Pruneda J.M., Artacho E., Dove M.T.* How the nature of the chemical bond governs resistance to amorphization by radiation damage // Phys. Rev. B. — 2005. — **71**, No 18. — P. 184104.

18. *Urusov V.S., Eremin N.N.* Charge — transfer energy in computer modelling of structure and properties of minerals // Phys. Chem. Miner. — 1997. — **24**, No 5. — P. 374—383.

19. *Wang S.X., Wang L.M., Ewing R.C., Doremus R.H.* Ion beam-induced amorphization in $MgO-Al2O_3-SiO_2$. I. Experimental and theoretical basis // J. Non-Cryst. Sol. — 1998. — **238**, No 3. — P. 198—213.

20. *http*://mpe.kmu.gov.ua/fuel/control/uk/publish/article?art_id=50310&cat_id=104126 (site of ministry of Fuel and Energy of Ukraine).

РЕЗЮМЕ. Радіаційна стійкість мінералів периклазу MgO, рутилу TiO_2, циркону $ZrSiO_4$, ксенотиму YPO_4, кварцу SiO_2, кристобаліту SiO_2, фосфату галію $GaPO_4$ та фторапатиту $Ca_{10}(PO_4)_6F_2$ досліджена за допомогою методів комп'ютерного моделювання. Кількість пар Френкеля, які формуються в структурі мінералу після проходження первинно вибитого атому торію з енергією 10 кеВ, розраховано за допомогою методу молекулярної динаміки. За методом *SIESTA* (теорія функціонала густини) проведені обчислення ступеня ковалентності хімічних зв'язків для цих мінералів. Обчислення ефективних зарядів атомів кисню проведені з використанням неемпіричного методу Хартрі-Фока та гібридного функціонала *B3LYP*. Встановлено, що радіаційна стійкість досліджених мінералів значною мірою залежить від топології структури (зв'язність структури, кількість різних поліедрів, що з'єднуються в позиціях атомів кисню, кількість нееквівалентних позицій атомів кисню та катіонів). Окрім того, радіаційна стійкість силікатів та оксидів металів значною мірою залежить від значень ефективних зарядів атомів кисню. Показано, що модуль об'ємної пружності мінералів також є важливим параметром, що впливає на радіаційну стійкість мінералів з однотипними структурами.

РЕЗЮМЕ. Радиационная устойчивость таких минералов, как периклаз MgO, рутил TiO_2, циркон $ZrSiO_4$, ксенотим YPO_4, кварц SiO_2, кристобалит SiO_2, фосфат галлия $GaPO_4$ и фторапатит $Ca_{10}(PO_4)_6F_2$ изучена с помощью методов компьютерного моделирования. Количество пар Френкеля, которые формируются в структуре минерала после прохождения первично выбитого атома тория с энергией 10 кэВ, рассчитано с помощью метода молекулярной динамики. По методу *SIESTA* (теория функционала плотности) проведены вычисления степени ковалентности химических связей для этих веществ. Неэмпирические расчеты методом Хартри-Фока с применением гибридного функционала *B3LYP* были выполнены для вычисления эффективных зарядов атомов кислорода в минералах. Установлено, что радиационная устойчивость исследованных минералов в значительной степени зависит от топологии структуры (связность структуры, количество различных полиэдров, которые соединяются в позициях атомов кислорода, количество неэквивалентных позиций атомов кислорода и катионов). Кроме того, радиационная устойчивость силикатов и оксидов металлов в значительной степени зависит от значений эффективных зарядов атомов кислорода. Показано, что модуль объемной упругости также служит важным параметром, влияющим на радиационную устойчивость минералов с однотипными структурами.